OXFORD

SOT | Society of Toxicology
www.toxsci.oxfordjournals.org

TOXICOLOGICAL SCIENCES, 156(2), 2017, 455–468

doi: 10.1093/toxsci/kfx009
Advance Access Publication Date: January 13, 2017
Research article

Vibrio cholerae Cholix Toxin-Induced HepG2 Cell Death is Enhanced by Tumor Necrosis Factor-Alpha Through ROS and Intracellular Signal-Regulated Kinases

Kohei Ogura,[*,†] Yasuhiro Terasaki,[‡] Tohru Miyoshi-Akiyama,[†] Mika Terasaki,[‡] Joel Moss,[§] Masatoshi Noda,[*] and Kinnosuke Yahiro[*,1]

[*]Department of Molecular Infectiology, Graduate School of Medicine, Chiba University, Chiba, Japan; [†]Pathogenic Microbe Laboratory, Research Institute, National Center for Global Health and Medicine, Tokyo, Japan; [‡]Department of Analytic Human Pathology, Nippon Medical School, Tokyo, Japan; and [§]Cardiovascular and Pulmonary Branch, National Heart, Lung, and Blood Institute, National Institutes of Health, Bethesda, Maryland 20892-1590

[1]To whom correspondence should be addressed at Department of Molecular Infectiology, Graduate School of Medicine, Chiba University, Chiba 2600856, Japan. Fax + (1) 81-43-226-2049. E-mail: yahirok@faculty.chiba-u.jp.

ABSTRACT

Cholix toxin (Cholix) from *Vibrio cholerae* is a potent virulence factor exhibiting ADP-ribosyltransferase activity on eukaryotic elongation factor 2 (eEF2) of host cells, resulting in the inhibition of protein synthesis. Administration of Cholix or its homologue *Pseudomonas* exotoxin A (PEA) to mice causes lethal hepatocyte damage. In this study, we demonstrate cytotoxicity of Cholix on human hepatocytes in the presence of tumor necrosis factor α (TNF-α), which has been reported to play a fatal role in PEA administered to mice. Compared with incubating HepG2 cells with Cholix alone, co-treatment with TNF-α and Cholix (TNF-α/Cholix) significantly enhanced the activation of caspases, cytochrome *c* release from mitochondria into cytoplasm, and poly-ADP-ribose polymerase (PARP) cleavage, while incubation with TNF-α alone or co-treatment with TNF-α/catalytically inactive Cholix did not. In the early stage of cell death, Cholix increased phosphorylation of mitogen-activated protein kinases (e.g., p38, ERK, JNK) and Akt, which was not affected by TNF-α alone. MAPK inhibitors (SP600125, SB20852, and U0126) suppressed PARP cleavage induced by TNF-α/Cholix. Protein kinase inhibitor Go6976 suppressed JNK phosphorylation and PARP cleavage by TNF-α/Cholix. In contrast, PKC activator PMA in the absence of TNF-α promoted Cholix-induced PARP cleavage. Reactive oxygen species (ROS) inhibitor, *N*-acetyl cysteine (NAC), suppressed TNF-α/Cholix-induced JNK and ERK phosphorylation, resulting in inhibition of PARP cleavage. These data suggest that ROS and JNK pathways are important mediators of TNF-α/Cholix-induced HepG2 cell death.

Key words: ADP-ribosyltransferase activity; tumor necrosis factor-alpha; ROS; toxin; cell death.

Vibrio cholerae (*V. cholerae*) is a Gram-negative bacterium transmitted to humans by water or food. Among more than 200 serogroups, based on surface O antigens of *V. cholerae*, only the O1 and O139 groups produce cholera toxin (CT) (Kaper *et al.*, 1995). Non-O1 and non-O139 *V. cholerae* strains have been isolated from patients with extra-intestinal infections (Hughes *et al.*, 1978; Morris and Black, 1985). Recent reports showed that Non-O1/non-O139 *V. cholerae* caused severe sepsis in a patient with underlying chronic liver disease (Khan *et al.*, 2013; Patel *et al.*, 2009). In early outbreaks of *V. cholerae* in Haiti during November 2010, pathogenic O1 and non-O1/O139 were found, respectively, in 48% and 21% of the samples, while O1 and non-O1/O139 were co-cultured from only 7% of the O1-positive samples (Hasan *et al.*, 2012).

Cholix toxin (Cholix) is a newly identified virulence factor in environmental non-O1, non-O139 *V. cholerae* strains. The

cholix gene was present in 47% of non-O1/non-O139 strains and 16% of O1/O139 strains in *V. cholerae* isolated in coastal waters of southern California (Purdy *et al.*, 2010). In another study, 27% of non-O1/non-O139 strains possessed *cholix* genes, which encoded toxins that varied in cytotoxicity, while O1 or O139 strains did not possess the gene (Awasthi *et al.*, 2013). Cholix is a 70-kDa protein toxin that translocates into cells by receptor-mediated endocytosis (Jorgensen *et al.*, 2008). It was identified as a novel virulence factor that catalyzes ADP-ribosylation of eukaryotic elongation factor 2 (eEF2). Cholix belongs to a group of eEF2 ADP-ribosylating toxins such as diphtheria toxin and *Pseudomonas* exotoxin A (PEA) from, respectively, *Corynebacterium diphtheriae* and *Pseudomonas aeruginosa*. These toxins specifically ADP-ribosylate diphthamide synthesized from a histidine residue by the diphthamide biosynthesis pathway, followed by inhibition of protein synthesis in host cells (Liu *et al.*, 2004; Roy *et al.*, 2010). Cholix exhibits significant homology to PEA, with a primary structural identity of about 35%. Previous studies have shown that PEA requires proteolytic cleavage by Furin, a Ca^{2+}-dependent serine protease, for induction of cytotoxic activity (Chiron *et al.*, 1997; Gu *et al.*, 1996; Inocencio *et al.*, 1994). Furin cleaves the consensus sequence -Arg-X-Lys/Arg-Arg- (RXK/RR) (Hosaka *et al.*, 1991). From crystal structure analysis, Cholix has a furin cleavage site at a translocation domain (domain II, 265–386) (Jorgensen *et al.*, 2008). We confirmed in HeLa cells that activation of Cholix required furin activity based on effects of a furin inhibitor (data not shown). Our previous data indicated that both Cholix and PEA induced caspase-dependent apoptosis in HeLa cells (Ogura *et al.*, 2011). PEA caused severe liver damage in mice (Iglewski *et al.*, 1977). PEA-induced liver injury in mice involved T cell-dependent Tumor necrosis factor α (TNF-α) production by Kupffer cells, which was mediated by TNF receptors TNFR1 and TNFR2 expressed in parenchyma, but not in leukocytes (Schumann *et al.*, 1998, 2000).

TNF-α, mainly produced by macrophages, contributes to a wide spectrum of human diseases and plays critical roles in inflammation and immunity (Parameswaran and Patial, 2010). TNF-α triggers apoptosis, necrosis, and survival signals through binding two different cell surface receptors, TNFR1 and TNFR2. Multiple experimental approaches have revealed that TNFR1 initiates the majority of TNF's biological activities (Chen and Goeddel, 2002). In TNFR1-mediated apoptosis, TNFR1-associated death domain protein (TRADD) recruits receptor-interacting protein 1 (RIP1) and Fas-associated death domain protein (FADD), leading to activation of caspases, followed by apoptosis (Baud and Karin, 2001; Croft *et al.*, 2012). Survival transcription pathways regulated by NF-κB in turn are induced by recruitment of TNF-receptor-associated factor 2 (TRAF2) and RIP by TRADD (Devin *et al.*, 2001; Zhang *et al.*, 2000). In addition to necrosis, TNF-α can induce programmed necrosis (necroptosis), which is initiated with deubiquitination of RIP1, destabilizing the TRADD–RIP1–FADD complex, and subsequent formation of complexes containing RIP1, RIP3, and caspase-8 (Cho *et al.*, 2009; Degterev *et al.*, 2005).

In Cholix-treated mice, inflammation and coagulation necrosis were observed in liver (Awasthi *et al.*, 2013). However, the mechanism of Cholix-induced hepatocyte death is unknown. In this report, we show that the pathways responsible for TNF-α-enhanced, Cholix-induced HepG2 cell death involves reactive oxygen species (ROS) and MAPK-dependent reactions.

MATERIALS AND METHODS

Preparation of Cholix Toxin

Cholix and its catalytically inactive mutant Cholix(E581A) were prepared as described in a previous report (Ogura et al., 2011). Briefly, pGEX-6P-1/Cholix or Cholix(E581A) plasmids were transfected into *E. coli* strain BL21(DE3). After induction with 0.5 mM IPTG (Wako Pure Chemical Industries) at room temperature overnight, expressed recombinant GST-tagged Cholix or Cholix(E581A) was applied to Glutathione Sepharose 4B (GE Healthcare). After washing the beads with phosphate-buffered saline (PBS) and digestion by PreScission Protease (GE Healthcare) at 4 °C overnight, the purified Cholix proteins were isolated from a flow-through fraction.

Cell Culture and Gene Silencing

HepG2 cells were maintained in Eagle's minimal essential medium (EMEM) (Sigma Aldrich), supplemented with 10% heat-inactivated fetal bovine serum, 100 U/ml penicillin, 100 μg/ml streptomycin (FBS-PCSM) and 1 mM sodium pyruvate (Sigma Aldrich). THP-1 cells were cultured in RPMI-1640 medium (Sigma Aldrich), supplemented with FBS-PCSM. Immortalized human hepatocytes, which were immortalized by transfection with the HCV core genomic region from genotype 1a (Ray *et al.*, 2000), were a gift from Tatsuro Kanda (Chiba University), and cultured in RPMI-1640 (Wako Pure Chemical Industries) supplemented with FBS-PCSM.

Non-targeting control (NC) siRNA was purchased from Sigma Aldrich. TNFR1 siRNA was synthesized according to a previous report (5′-CAA AGG AAC CUA CUU GUA CUU-3′) (Cho *et al.*, 2008). HepG2 cells (2×10^5 cells) in a 24-well dish were cultivated overnight in EMEM containing 10% FBS and 1 mM sodium pyruvate and transfected for 48 h with the indicated siRNA (100 nM) using DharmaFECT 4 Transfection Reagent (Dharmacon) in OPTI-MEM I reduced serum medium (GIBCO/Invitrogen), according to the protocol of the manufacturer. Transfection efficiency and effect were evaluated by Western blotting using the indicated antibodies.

Double Chamber Cell Culture System

Briefly, HepG2 cells (2×10^5 cells/well) were seeded in lower wells and PMA-differentiated THP-1 cells (2×10^5 cells/well) were cultured in the upper chamber on PET-track-etched membrane (0.4 μM) (BD Bioscience). The toxins (10 μg/ml) were added to the upper or lower chamber medium for 12 h at 37 °C, and then cell lysates were prepared for Western blot analysis.

Reagents

A general caspase inhibitor (Z-VAD-FMK) was purchased from BD Biosciences, p38 inhibitor SB2003580 from Wako Pure Chemical Industries, MEK inhibitor U0126 and PKC inhibitor Go6973 from LC Laboratories, Inc., c-Jun kinase (JNK) inhibitor SP600125, JAK2 inhibitor Ruxolitinib, Flt3 inhibitor Quizartinib, and PKC inhibitor Go6983 from Cayman Chemical, PKC inhibitor Bisindolylmaleimide II (Bis II) and Furin inhibitor I from ALEXIS Biochemicals, and PKC activator PMA, Trk inhibitor GNF5837, CID755673, and *N*-acetyl cysteine (NAC) from Sigma Aldrich. For Western blot analysis, anti-cleaved caspases-3 (9661), anti-cleaved caspase-6 (D162), anti-cleaved caspase-7 (9491S), anti-cleaved caspase-8 (9496S), anti-cleaved caspase-9 (9501), anti-cleaved PARP (9542), anti-cleaved PARP mouse

specific (9544), anti-phospho-p38 MAPK (Thr180/Tyr182) (9211S), and anti-phospho-p44/42 MAPK (Erk1/2) (Thr202/Tyr204) (4370S) antibodies were purchased from Cell Signaling Technology; anti-JNK (610627), anti-phospho-JNK (pT183/pY185) (612540), anti-p38 (612168) MAPK, and anti-Erk1 (610030) antibodies were from BD Bioscience; anti-hTNF R1 (AF225) antibody from R&D SYSTEMS; anti-cytochrome *c* (sc-13560) antibodies from Santa Cruz Biotechnology; anti-GAPDH (GTX100118) antibody from GeneTex; and anti-α-Tubulin antibody (T90260) from Sigma Aldrich; anti-β-actin (bs-0061R) antibody from Bioss. HRP-conjugated anti-mouse IgG (HAF007) and anti-rabbit IgG (HAF008) antibodies were purchased from R&D Systems.

Animals

All animal experiments were approved by the National Center for Global Health and Medicine Ethical Committee and Chiba University Institutional Animal Care and Use Committee (Japan). Male C57BL/6J mice (Japan SLC), 6–8 weeks old, were injected intraperitoneally (I.P.) with purified wild-type Cholix, mutant Cholix (2 mg/kg) or PBS as a control. The organs were perfusion-fixed, removed, and fixed in 20% formalin neutral buffer solution (Wako Pure Chemical Industries) for 24 h at room temperature, embedded in paraffin, sectioned, stained with Periodic acid-Schiff (PAS), hematoxylin–eosin (HE), and terminal deoxynucleotidyl transferase dUTP nick-end labeling (TUNEL) and examined by light microscopy. Serum alanine transaminase levels were measured by a standard method at Oriental Kobo Life Science Laboratory.

Western Blot Analysis

Mouse livers were homogenized by Multi-Beads Shocker (Yasui-kikai) in RIPA buffer (10 mM Tris-Cl pH 8.0, 1 mM EDTA, 1% Triton X-100, 0.1% sodium deoxycholate, 0.1% SDS, and 140 mM NaCl). After centrifugation, supernatants were utilized for Western blot analysis. Total cell lysate or cytosolic fraction of the cell line was obtained according to previous reports (Chen *et al.*, 2007; Morinaga *et al.*, 2008). HRP-bound protein bands were detected by Super Signal West Pico mixture (Thermo Scientific) and visualized by Las-1000 (Fuji Film).

RNA Isolation and RT-PCR

Total RNA were extracted from HepG2 cells at the indicated time points following incubation with wild type Cholix or mutant Cholix using ISOGEN II (NIPPON GENE) according to the instructions from the manufacturer. Complementary DNA (cDNA) was synthesized from 5μg of total RNA using PrimeScript™ 1st strand cDNA Synthesis Kit (TaKaRa Bio Inc.). cDNA was amplified using rTaq polymerase (TaKaRa Bio Inc.) in a 25 μl PCR mixture according to the protocol of the manufacturer. The PCR conditions were as follows: 30 cycles of 98 °C for 10s, 55 °C for 30s, and 72 °C for 60s. Primers used for PCR (Burvall *et al.*, 2005) were as follows: TNFR1, 5′-ACC AAG TGC CAC AAA GGA AC-3′ (forward) and 5′-CTG CAA TTG AAG CAC TGG AA-3′ (reverse); TNFR2, 5′-TTC GCT CTT CCA GTT GGA CT-3′ (forward) and 5′-CAC CAG GGG AAG AAT CTG AG-3′ (reverse); GAPDH, 5′-TGAAGGTCGGAGTCAACGGATTTGGT-3′ (forward) and 5′-CATGTGGGCCATGAGGTCCACCAC-3’ (reverse). PCR products were subjected to electrophoresis on 2% agarose gels containing ethidium bromide, and the bands were visualized under ultraviolet (UV) light.

Cell Viability Assay

Cells (1×10^4 cells/well) were treated with TNF-α and/or Cholix for 24 h in the presence or absence of the indicated inhibitors. Cell viability was determined by Cell Counting Kit (Dojindo Molecular Technologies Inc.), which is based on colorimetric quantification of NADH.

Detection of ATP Levels

For measurement of ATP level in HepG2 cells, we used Luminescent ATP Detection Assay Kit (Abcam) according to the protocol of the manufacturer. Briefly, cells were incubated with wild-type Cholix or Cholix(E581A) mutant in the presence or absence of TNF-α for 18 h. ATP in the cell lysates was measured by luciferase activity using the GloMAX-Multi Detection System (Promega).

RESULTS

Administration of Cholix to Mice Results in Hepatic Damage

We first examined the effect of Cholix in mice. Intraperitoneal injection of Cholix, but not catalytically inactive mutant Cholix(E581A), resulted in death within 24 h. We observed a marked decrease in Periodic acid-Schiff (PAS)-positive hepatocytes in Cholix-injected mice (Figure 1A-d, -e, and -f), indicating that glycogen-positive normal hepatocytes were damaged, as compared with control PBS or mutant Cholix-treated mice. In agreement with a previous report (Awasthi *et al.*, 2013), we also found degenerated destructive and hemorrhagic lesions with apoptotic and inflammatory cells especially at the liver zone between Glisson's sheath and central vein by PAS and HE staining in Cholix-injected mice (Figure 1A-d, -e, and -f) compared with control PBS (Figure 1A-a, -b, and -c) or mutant Cholix-treated mice (Figure 1A-g, -h, and -i). These histological features reveal that Cholix causes lethality with severe liver damage and hepatocyte death. We next investigated the liver injury in Cholix-injected mice in a time-dependent manner. The liver lysate of Cholix-injected mice showed cleavage of poly (ADP-ribose) polymerase (PARP), a marker of apoptosis, after 18 h, but PBS or the mutant Cholix(E581A) did not (Figure 1B). Furthermore, we assessed serum alanine transaminase (ALT) to determine liver damage. As shown in Figure 1C, ALT was significantly increased in Cholix-, but not mutant Cholix(E581A)-, injected mice after 18 h. These results indicated that Cholix is a lethal factor causing liver injury.

Effect of TNF-α on Cholix-Induced Cell Death

Previous studies showed that PEA-induced liver damage involved TNF-α production by Kupffer cells (Schumann *et al.*, 1998, 2000). We investigated the effect of TNF-α on Cholix-induced cytotoxicity in various cells in the presence or absence of TNF-α for 24 h (Figure 2A and Supplementary Figure 1). In THP-1 cells, TNF-α, but not Cholix, decreased the cell viability (Supplementary Figure 1). In HepG2 cells, Cholix slightly decreased cell viability. TNF-α treatment alone did not affect HepG2 cell viability. Co-treatment of cells with TNF-α/Cholix dramatically decreased viability (20%–40%) (Figure 2A). Consistent with cell viability data, in HepG2 cells, TNF-α/Cholix, but not TNF-α alone or TNF-α/Cholix(E581A), significantly decreased cellular ATP levels (Figure 2B). To explore the mechanism of Cholix-induced cell death in HepG2 cells, we

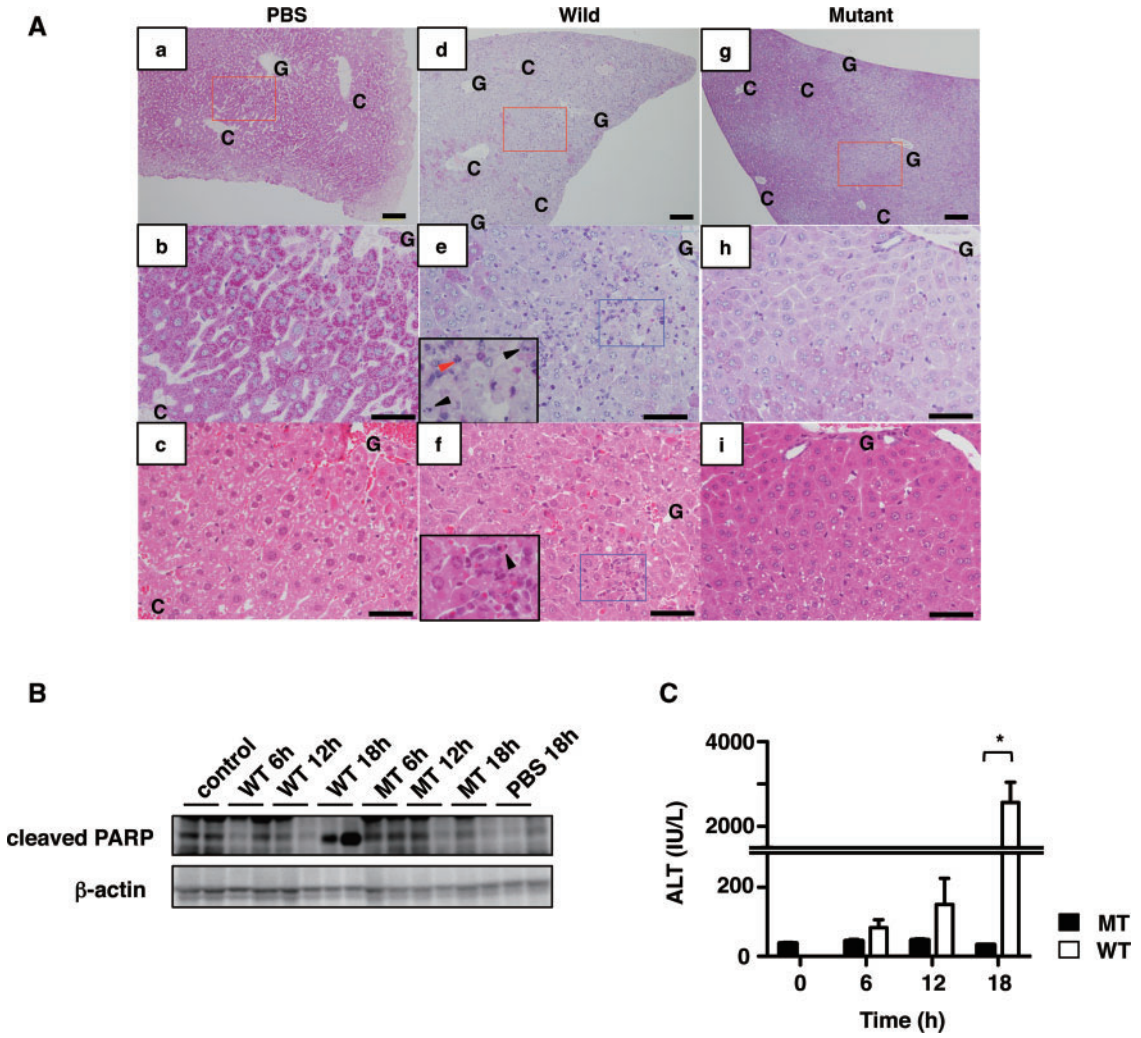

FIG. 1. Characterization of livers from mice treated with Cholix. A, Representative liver images stained by Periodic acid-Schiff: PAS (a, b, d, e, g, h) or hematoxylin–eosin: HE (c, f, i) from mice treated with PBS control (a-c), wild-type Cholix (d–f), and mutant-type Cholix (g–i) for 24 h. b, e, and h show high-magnification views of the red rectangular areas in a, d, and g, respectively. Paired images of b/c, e/f and h/i are the same areas stained by PAS/HE with serial sections, respectively. Insets in e or f show high-magnification views of damaged liver with apoptotic cells (arrowheads) and granulocytes (red arrowhead) in the blue rectangular areas of e or f respectively. Scale bars = 100 μm (a, d, c) and 50 μm (b, c, e, f, h, i). C and G, indicate central vein and Glisson's sheath, respectively. B and C, Time-course of Cholix-injected mice. Mice were injected I.P. with PBS (n=3), wild-type Cholix (n=4), and mutant Cholix(E581A) (n=3). Liver and serum were obtained from each mouse at the indicated times, and then PARP cleavage in the liver (B) and serum ALT level (C) were determined as described in Materials and Methods section. Two representative samples from three mice of each group were utilized for immunoblotting. C, Average and standard deviations of serum ALT levels in each group is shown and significance is *$P < 0.01$. The black bar indicates mutant Cholix(E581A) (MT) and white bar is wild-type Cholix (WT).

investigated the time dependence of PARP cleavage and caspase activation (Figure 2C and Supplementary Figure 2C). In the absence of TNF-α after 18–24 h treatment, Cholix induced activation of caspase (e.g., caspase-3, -7, -8, -9), PARP cleavage, and cytochrome *c* release. Treatment of cells with TNF-α/Cholix showed that compared with Cholix alone, caspase activation, PARP cleavage, and cytochrome *c* release were observed at early time points (12 h) and increased at 12–24 h. Treatment of cells with mutant Cholix(E581A) or TNF-α/Cholix(E581A) did not induce these signals. These data suggested that addition of TNF-α accelerates and enhances apoptotic signals induced by Cholix.

Effects of Caspase and Akt Inhibitors on HepG2 Apoptosis and Necrosis

We next examined effects of a general caspase inhibitor Z-VAD-Fmk on TNF-α/Cholix-induced cell death. Pretreatment with a general caspase inhibitor Z-VAD-Fmk significantly suppressed TNF-α/Cholix-induced activation of caspases-3, -7, and -8, and PARP cleavage (Figure 3A). We next investigated cell viability with or without general caspase inhibitor Z-VAD-Fmk and/or necrosis inhibitor Necrostain-1. Cholix/TNF-α-induced decrease in cell viability was dramatically reversed by both Necrostatin-1 and Z-VAD-Fmk, but not by Z-VAD-Fmk alone or Necrostain-1 alone (Figure 3B). These data indicated that Cholix-mediated HepG2 cell death is enhanced by TNF-α, and involves both caspase- and necrosis-dependent pathways.

These inhibitors partially reversed the loss of cell viability (Figure 3B), indicating that HepG2 cell death induced by TNF-α/Cholix is associated with activation of apoptotic and other pathways. As shown in Figure 3C, Cholix induced Akt phosphorylation, which was increased by TNF-α at the basal level. In the presence of Akt inhibitor Akti, Cholix-induced Akt (Ser473) phosphorylation was significantly suppressed. Under these conditions, in TNF-α/Cholix-treated HepG2 cells, pretreatment with Akti resulted in increased apoptotic signals and decreased cell

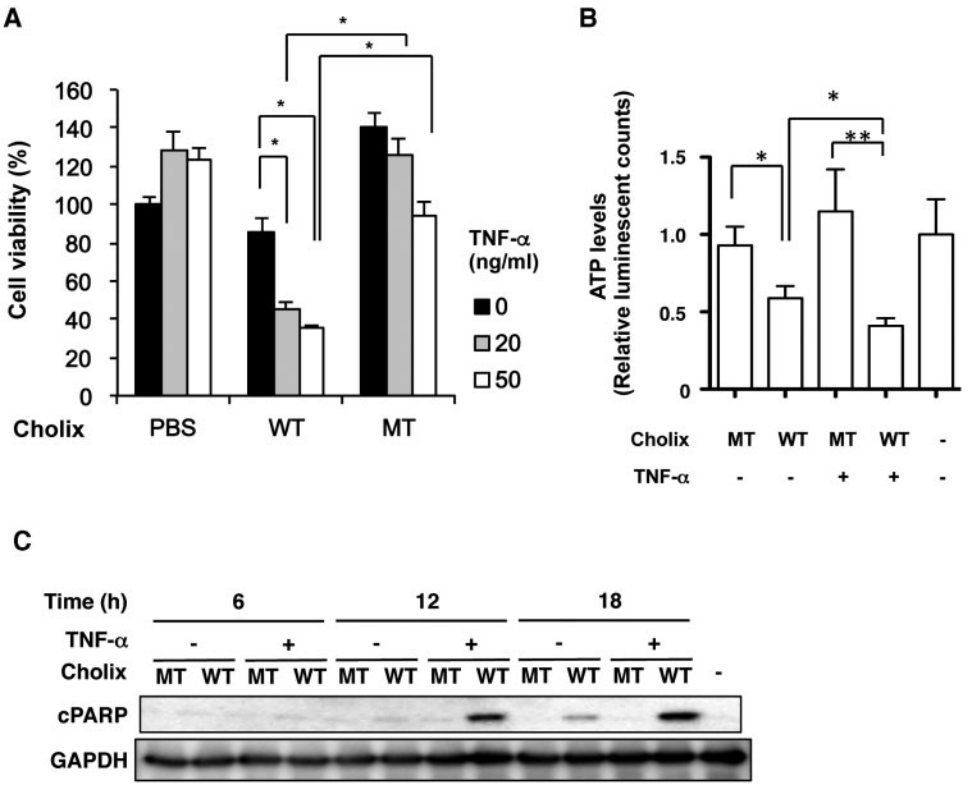

FIG. 2. Effect of Cholix and TNF-α on cell viability. **A,** HepG2 cells were treated for 48 h with PBS (control), 10 μg/ml wild-type Cholix (WT), or mutant Cholix(E581A) (MT) in the presence or absence of TNF-α (0, 20, 50 ng/ml). Cell viability was measured using Cell Counting Kit. Data are the means ± SD from three separate triplicate experiments. Student's *t*-test was utilized for comparisons with untreated cells and significance is *$P < 0.01$. B, HepG2 cells (3×10^4 cells/well) were treated with PBS (−), 10 μg/ml wild-type Cholix (WT), or mutant Cholix(E581A) (MT) in the presence or absence of TNF-α (25 ng/ml). The ATP level was measured using Luminescent ATP Detection Assay Kit according to the protocol of the manufacturer as described in Materials and Methods section. Data are the means ± SD from two separate triplicate experiments. Student's *t*-test was utilized for comparisons with untreated cells and significance is *$P<0.005$ and ** $P<0.01$, respectively. C, HepG2 cells (2×10^5 cells/well) were treated with 10 μg/ml wild-type Cholix (WT) or mutant Cholix(E581A) (MT) in presence or absence of TNF-α (25 ng/ml) for the indicated times. Then, cells were lysed with 1×SDS sample buffer for immunoblotting with the indicated antibodies. Experiments were repeated three times with similar results.

viability (Figure 3D and E). However, co-pretreatment with Akti and Z-VAD-Fmk improved cell viability (Figure 3E). Further, pretreatment HepG2 cells with JNK inhibitor SP600125 suppressed Cholix-induced Akt phosphorylation (Supplementary Figure 3). These results suggested that TNF-α/Cholix induces both Akt- and caspase- dependent HepG2 cell death, and Akt phosphorylation is downstream of JNK signaling.

Cholix Induced Apoptosis in HepG2 Cells Co-Cultured With Macrophage-like THP-1 Cells

We next examined whether human macrophages participate in hepatocyte death through TNF-α production. As shown in Figure 4A, the two different types of cells used in the *in vitro* co-culture system, although not directly in contact, indirectly crosstalk via soluble factors produced by each. Monocytic THP-1 cells or macrophage-like THP-1 cells differentiated by PMA were cultured on a semipermeable membrane, and HepG2 cells were seeded in bottom plates. We added the toxins to the apical or basolateral media. The amounts of TNF-α in both membrane and soluble form were increased in macrophage-like THP-1 cells. After 12 h incubation, Cholix-induced PARP cleavage and caspase-6 activation were only detected in HepG2 cells when Cholix was added to the basolateral side and co-cultured with macrophage-like THP-1 cells (Figure 4B). In addition, Cholix treatment did not promote PARP cleavage or TNF-α production by the monocytic THP-1 cells or differentiated macrophage-like THP-1. Cholix-induced PARP cleavage in HepG2 cells was not induced by Cholix treatment on the apical side (Figure 4B). A previous report showed that TNF receptor 1 (TNFR1) was activated by soluble TNF-α and TNFR2 activation was required for interaction with membrane form of TNF-α (Wajant *et al.*, 2003). By RT-PCR analysis, we determined the expression levels of TNFR1 and TNFR2. TNFR1, not TNFR2, was the primary form expressed in HepG2 cells and it was expressed in HepG2 cells and not increased by Cholix (Figure 4C). We next investigated the effect of TNFR1 on TNF-α/Cholix-induced PARP cleavage. Cholix decreased the amount of TNFR1 in HepG2 cells. Knockdown of TNFR1 by siRNA significantly suppressed TNF-α/Cholix-induced PARP cleavage compared with the control siRNA-transfected cells (Figure 4D). Further, the amount of TNFR1 was decreased by Cholix, but not Cholix(E581A). Proteasome inhibitor, lactacystin, inhibited Cholix-decreased TNFR1 expression, which was not affected by lysosome inhibitor, Chloroquine. Thus, TNFR1 was rapidly degraded by proteasomes in the presence of Cholix (Figure 4E). These results indicated that soluble TNF-α from macrophage-like THP-1 cells is an essential factor for enhancement of Cholix-induced HepG2 cell death via TNFR1.

Cholix Activates MAPK Pathways in HepG2 Cells

We found that after 8 h incubation, Cholix, but not Cholix(E581A), induced phosphorylation of p38, ERK, and JNK.

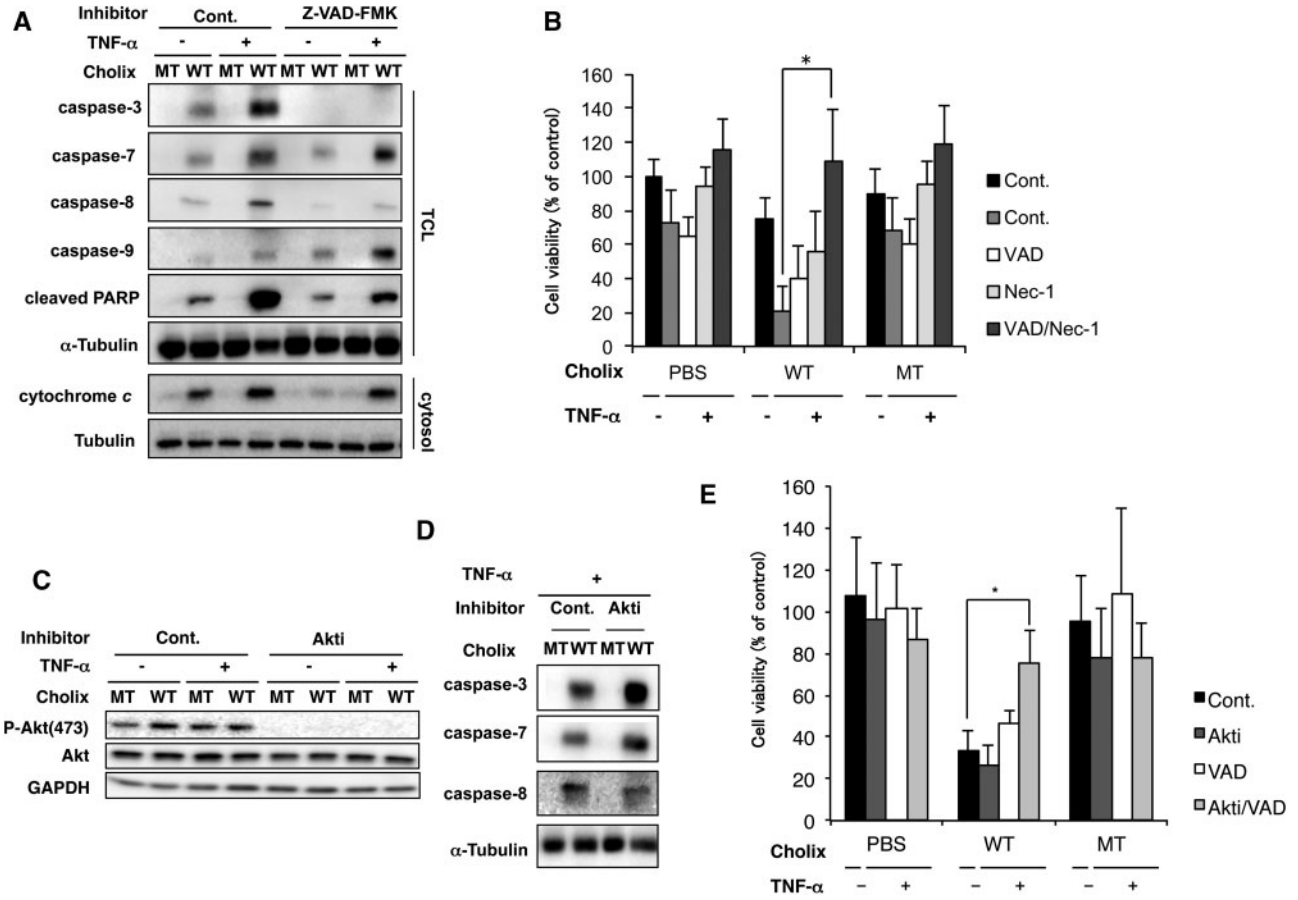

FIG. 3. TNF-α/Cholix-induced cell death is inhibited by both Z-VAD-Fmk and Necrostatin-1. **A,** HepG2 cells (2×10^5 cells/well) were treated for 30 min with or without 25 μM Z-VAD-Fmk, and then incubated for 18 h with 10 μg/ml wild-type Cholix (WT) or mutant Cholix(E581A) (MT) in the presence or absence of TNF-α (25 ng/ml). These cells were lysed with 1×SDS sample buffer for immunoblotting with the indicated antibodies. Experiments were repeated three times with similar results. B, HepG2 cells (1×10^4 cells/well) were treated for 30 min with or without Z-VAD-Fmk (VAD) and/or Necrostatin-1 (Nec-1), and then incubated for 24 h with 10 μg/ml wild-type Cholix (WT), or inactivated mutant Cholix(E581A) (MT) in the absence or presence of 25 ng/ml TNF-α. Cell viability was measured using Cell Counting Kit. Data are the means ± SD from three separate triplicate experiments. Student's *t*-test was utilized for comparisons with the untreated cells and significance is $^*P < 0.01$. **C** and D, HepG2 cells (2×10^5 cells/well) were treated for 30 min with or without 5 μM Akti-1/2, and then incubated for 18 h with WT or MT Cholix in the presence of TNF-α (25 ng/ml). Cells were lysed with 1×SDS sample buffer for immunoblotting with the indicated antibodies. Experiments were repeated three times with similar results. E, HepG2 cells (1×10^4 cells/well) were treated for 30 min with or without 5 μM Akti-1/2 and/or Z-VAD-Fmk (VAD), and then incubated for 24 h with 10 μg/ml WT or MT Cholix in the absence or presence of 25 ng/ml TNF-α. Cell viability was measured using Cell Counting Kit. Data are the means ± SD from three separate triplicate experiments. Student's *t*-test was utilized for comparisons with the untreated cells and significance is $^*P < 0.01$.

TNF-α did not significantly affect Cholix-induced phosphorylation of p38, ERK, and JNK, suggesting that a TNF-α signal is not essential for activation of MAPKs (Figure 5A). To investigate if Cholix-activated MAPK pathways participated in cell death, we used specific inhibitors (e.g., SB203580, U0126, SP600125), followed by assessment of apoptotic signals. PARP cleavage by TNF-α/Cholix was suppressed by pretreatment with U0126 or SP600125, but not by SB203580 (Figure 5B). SP600125 did not affect Cholix-induced phosphorylation of ERK and p38. U0126 suppressed Cholix-induced phosphorylation of JNK, ERK, and p38, which were not altered by SB203580. Thus, Cholix-induced ERK activation is upstream of p38 and JNK activation. These results suggest that MAPKs regulate TNF-α/Cholix-induced apoptosis.

PKC Inhibitor Go6973 Inhibits TNF-α/Cholix-Induced PARP Cleavage

It has been reported that TNF-α-induced cell death is mediated by protein kinase C (PKC) isoforms (Chang and Tepperman, 2001). We next investigated the effect of PKC inhibitors (e.g., Bisindolylmaleimide II, Go6976, Go6983) on TNF-α/Cholix-enhanced cell death. These compounds commonly inhibit PKCα and PKCβ. Go6976, but not other PKC inhibitors, significantly inhibited TNF-α/Cholix-induced PARP cleavage (Figure 6A). Pretreatment of HepG2 cells with phorbol 12-myristate 13-acetate (PMA) in the absence of TNF-α promoted Cholix-induced PARP cleavage . A similar effect was seen with TNF-α/Cholix (Figure 6B). Go6976 is known to inhibit PKCα, β and μ as well as JAK2, Trk, and Flt3 (Behrens *et al.*, 1999; Grandage *et al.*, 2006; Gschwendt *et al.*, 1996; Martiny-Baron *et al.*, 1993). PKCμ inhibitor, CID755673, did not inhibit Cholix/TNF-α-induced PARP cleavage (Supplementary Figure 1). Inhibitors of JAK2 (Ruxolitinib), Flt3 (Quizartinib), and Trk (GNF5867) did not suppress Cholix/TNF-α-induced PARP cleavage (Figure 6C and D). Previous study has shown that Go6976 prevented JNK activation (Lopez-Bergami *et al.*, 2005). Pretreatment of HepG2 cells with Go6976 inhibited Cholix/TNF-α-increased phosphorylation of JNK and ERK, but did not alter p38 phosphorylation. Bisindolylmaleimide II did not affect MAPK phosphorylation increased by Cholix/TNF-α (Figure 6E).

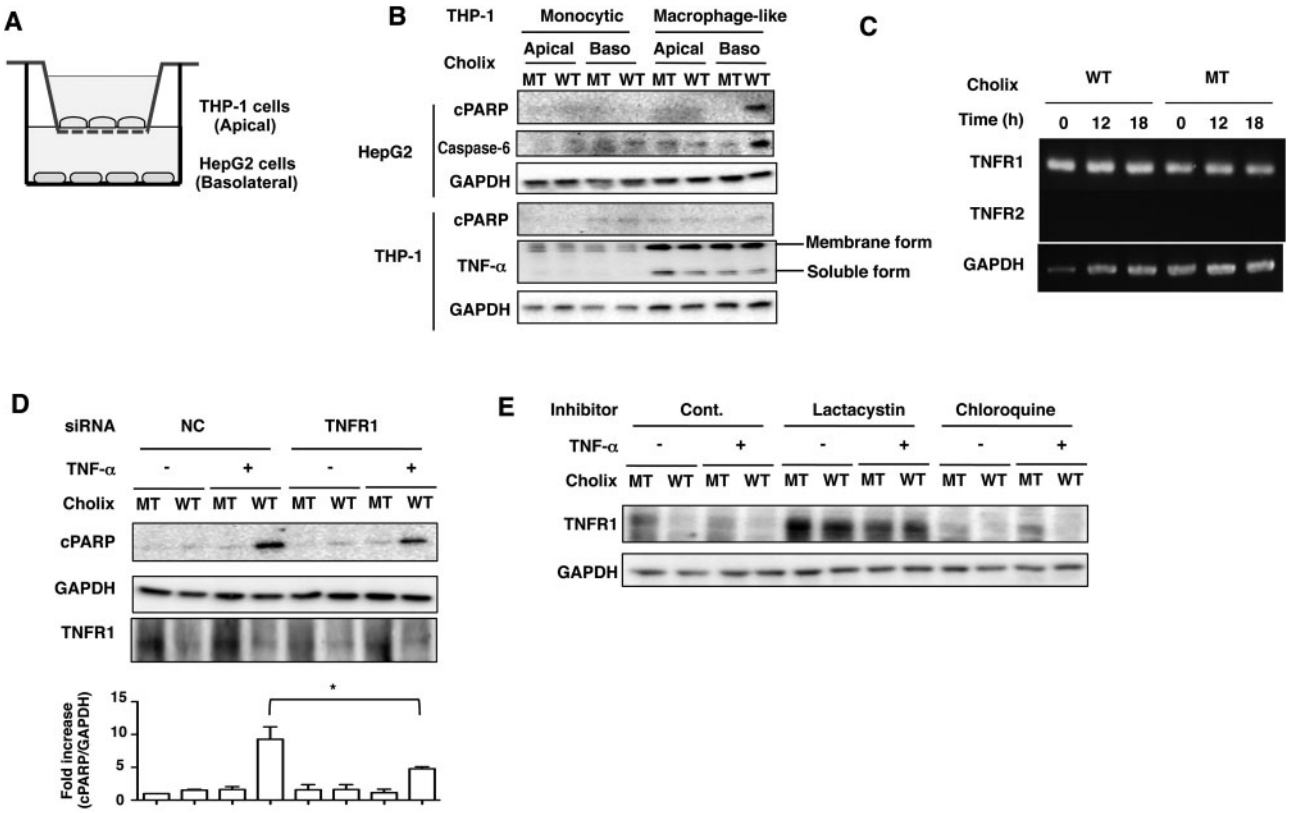

FIG. 4. Apoptotic signals are induced by Cholix in the co-culture system. **A,** Schematic drawing of co-culture system. Confluent THP-1 cells or PMA-differentiated macrophage-like cells were plated on apical side (Apical), which has a semipermeable membrane. HepG2 cells (1×10^4 cells/well) were plated on basolateral side (Baso) and the system was cultured overnight. **B,** Cholix (10 μg/ml) was added to the apical or basolateral media and the cells were incubated for 12 h and then collected. Then, cells were lysed with 1×SDS sample buffer for immunoblotting with the indicated antibodies. Experiments were repeated three times with similar results. **C,** HepG2 cells were incubated with mutant or wild-type Cholix for 0, 12, 18 h, and then total RNA was extracted. Expression of TNFR1, TNFR2, and GAPDH mRNA was detected by RT-PCR as described in Materials and Methods section. **D,** The indicated siRNA-transfected HepG2 cells were incubated for 12 h with 10 μg/ml wild-type Cholix (WT) or mutant Cholix(E581A) (MT)in the presence or absence of TNF-α (25 ng/ml). Then, cells were lysed with 1×SDS sample buffer for immunoblotting with the indicated antibodies. Experiments were repeated three times with similar results. Quantification of TNF-α/Cholix-induced PARP cleavage was performed by densitometry (bottom panel). Data are presented as mean ±SD of values from three experiments and significance is $^*P<0.05$. **E,** Cells were treated for 30 min with or without 10 μM lactacystin or 100 μM chloroquine, and then incubated for 12 h with 10 μg/ml wild-type Cholix (WT) or mutant Cholix (MT) in the presence or absence of TNF-α (25 ng/ml). Cells were lysed with 1×SDS sample buffer for immunoblotting with the indicated antibodies. A blot representative of three separate experiments is shown.

ROS Inhibitor Inhibits TNF-α/Cholix-Induced Apoptotic Signals in HepG2 Cells

To examine the effects of ROS on TNF-α/Cholix-induced HepG2 cell death, we used ROS inhibitor *N*-acetyl cysteine (NAC), followed by assessment of apoptotic signals. After pretreatment of cells with NAC, TNF-α/Cholix-induced caspase-7 and -8 activation and PARP cleavage was suppressed (Figure 7A). Next, we investigated the effect of NAC on Cholix-induced MAP kinase activation. NAC suppressed Cholix-mediated phosphorylation of p38, JNK, and Akt, but not ERK (Figure 7B). These data suggest that, in HepG2 cells, ROS production by TNF-α/Cholix initiates MAP kinase activation, followed by the induction of apoptotic signals.

Cholix-Induced PARP Cleavage is Not Enhanced by TNF-α in Immortalized Human Hepatocytes

To investigate the effect of Cholix with or without TNF-α on immortalized human hepatocytes, cells were pretreated with NAC, SP600125, Go6976, or Akti, followed by assessment of apoptotic signals (Figure 8A–D). Unlike HepG2 cells, TNF-α did not promote Cholix-induced PARP cleavage, which was enhanced by NAC and Akti (Figure 8A and D). Further, Cholix suppressed Akt phosphorylation. After pretreatment of cells with SP600125 or Go6976, Cholix-induced PARP cleavage was suppressed as was seen in HepG2 cells. These findings suggest that immortalized human hepatocytes are more sensitive to Cholix compared with HepG2 cells and that Cholix-induced cell death mechanism is different between HepG2 cells and immortalized human hepatocytes. Cholix-induced apoptosis is independent of TNF-α and ROS in immortalized human hepatocytes. Further, Cholix action is regulated in immortalized human hepatocytes by a JNK-dependent signaling pathway.

DISCUSSION

We demonstrate here that intraperitoneal injection of Cholix to mice caused a lethal, hemorrhagic inflammation and cytotoxic response in liver within 24 h (Figure 1). In Cholix-treated mouse liver, we found PARP cleavage after 18 h and some TUNEL-positive cells (Supplementary Figure 2). The mechanism by which Cholix induced hepatic cell death remains unknown. To date, only one report has shown *in vivo* cytotoxicity of Cholix (Awasthi *et al.*, 2013). Cholix exhibits high homology to PEA with a primary structural identity of about 35% (Jorgensen *et al.*, 2008). It was reported that PEA induced hepatic injury, which is

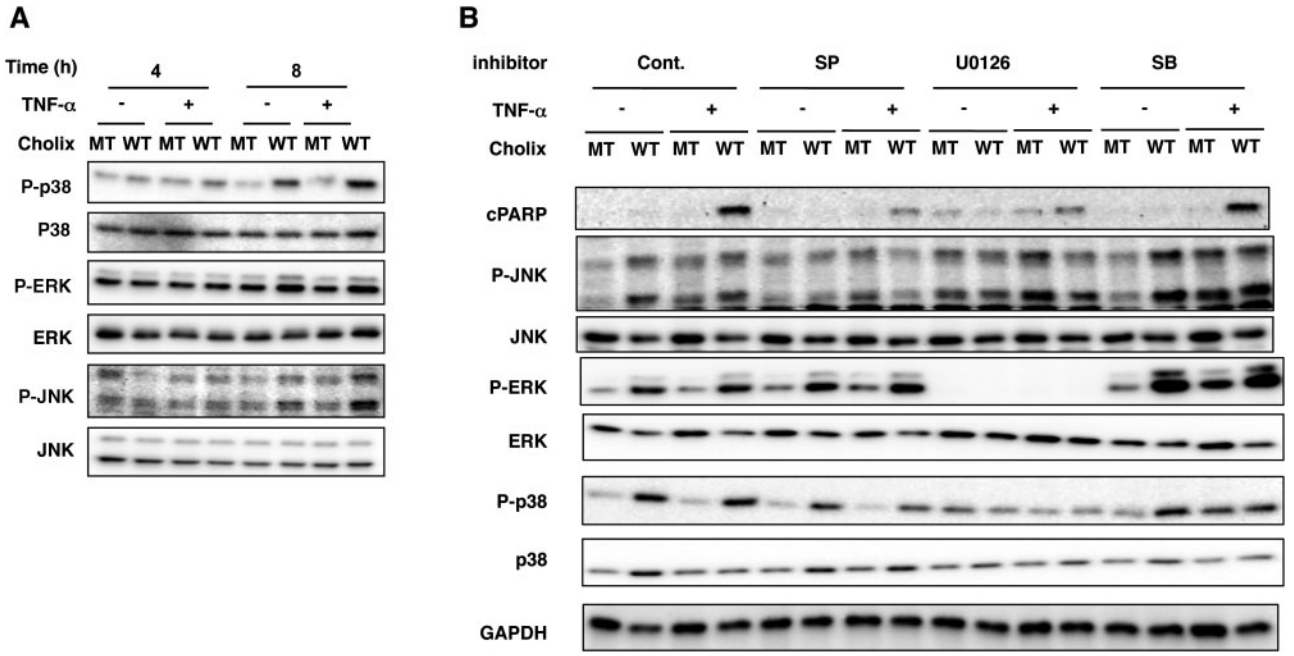

FIG. 5. Effect of TNF-α/Cholix on MAP kinases in HepG2 cells. A, Time course of MAP kinase phosphorylation induced by TNF-α and Cholix. HepG2 cells (2×10^5 cells/well) in 48-well plates were incubated with 10 μg/ml wild-type Cholix (WT) or mutant Cholix(E581A) (MT) in the presence or absence of TNF-α (25 ng/ml) for the indicated times. Then, cells were lysed with 1×SDS sample buffer for immunoblotting with the indicated antibodies. Experiments were repeated three times with similar results. B, Effect of MAPK inhibitors on MAPK phosphorylation and apoptotic signals induced by TNF-α/Cholix. HepG2 cells were treated for 30 min with 10 μM SP600125 (SP), 10 μM U0126 or 20 μM SB20350 (SB), followed by incubation for 12 h with 10 μg/ml wild-type Cholix (WT) or mutant Cholix (MT) in the presence or absence of TNF-α (25 ng/ml). Then, cells were lysed with 1×SDS sample buffer for immunoblotting with the indicated antibodies. Experiments were repeated three times with similar results.

mediated by TNF-α produced by Kupffer cells (Schumann *et al.*, 1998, 2000). In a rat model, massive necrosis and apoptosis were induced by injection of PEA, while only apoptotic cells were observed at lower dose (Chiu *et al.*, 2009).

As shown in Figure 2 and 8, and a previous report (Ogura *et al.*, 2011), sensitivity of human cell lines to Cholix was variable. In the presence of TNF-α, Cholix, but not the catalytically inactive mutant Cholix(E581A), induced accelerated cell death in HepG2 cells. Liedtke *et al.* (2002) reported that human hepatocyte Huh7 cells co-treated with TNF-α and cycloheximide undergo apoptosis, preceded by JNK activation. Cholix-induced PARP cleavage was detected in Huh7 cells (data not shown) and immortalized human hepatocytes in the absence of TNF-α (Figure 8), similar to the observation in HeLa cells (Ogura *et al.*, 2011), suggesting that the apoptotic pathway induced by TNF-α/cycloheximide is different from that activated by Cholix.

In TNF-α/Cholix-treated HepG2 cells, apoptotic signals were activated after a 12-h incubation (Figure 2C). Pretreatment with a general caspase inhibitor suppressed TNF-α/Cholix-induced activation of caspase-3 and caspase-8. However, the inhibitor did not completely suppress cytochrome *c* release and activation of caspase-7 and caspase-9. These findings suggest that TNF-α/Cholix-induced cytochrome *c* release from mitochondria is caspase-independent, but is followed by caspase-9 and -7 activation. We previously found in HeLa cells that Cholix induced caspase-mediated apoptosis dependent on inflammatory caspases and caspase-8 (Ogura *et al.*, 2011). As shown in Figure 7, inhibition of ROS signals by NAC significantly suppressed apoptosis in TNF-α/Cholix-treated HepG2, while NAC did not suppress apoptosis in Cholix-treated human immortalized hepatocytes (Figure 8), suggesting that Cholix-induced apoptosis has TNF-α-initiated ROS- and non-ROS-dependent pathways.

It is known that TNF-α is involved in liver injury (Schwabe and Brenner, 2006). In a co-culture system as shown in Figure 4, PMA-induced differentiation of the THP-1 monocytic cells to a macrophage-like cells resulted in increased expression of membrane and soluble forms of TNF-α. Cholix did not enhance TNF-α production in macrophage-like THP-1 cells. When Cholix was added to the apical side, it was absorbed to THP-1 cells, and, therefore, might not reach HepG2 cells in the bottom chamber. In contrast, addition of Cholix to the basolateral side allowed contact with TNF-α-stimulated HepG2 cells, resulting in enhanced Cholix-induced PARP cleavage and caspase activation. Previous studies showed that PEA-induced TNF-α production in Kupffer cells was activated by T cells (Muhlen *et al.*, 2004; Schumann *et al.*, 1998). Thus, Cholix did not directly induce TNF-α production by macrophages but acted through signals from other cells to macrophages, resulting in liver injury *in vivo*.

TNFR1 is the predominant TNF receptor expressed by HepG2 cells. Cholix down-regulated the amount of TNFR1, although TNFR1 mRNA expression was not changed by Cholix. TNF-α-TNFR1 complexes are rapidly endocytosed by cells and then degraded in secondary lysosomes to terminate signaling (Mosselmans *et al.*, 1988). Another group demonstrated that TNFR1 internalized by adenovirus RIDα/β was degraded through the endosomal/lysosomal pathway (Chin and Horwitz, 2005). However, TNFR1 expression in TNF-α/Cholix(E581A) mutant-treated cells was similar to that in cells treated with Cholix(E581A) mutant alone. In agreement, in HepG2 cells, complex formation between TNF-α and TNFR1 did not affect TNFR1 expression on the cell surface. Pretreatment of HepG2 cells with a proteasome inhibitor, lactacystin, blocked down-regulation of TNFR1 expression by Cholix, although it was not affected by the lysosome inhibitor chloroquine (Figure 4). These data suggest that the Cholix-dependent decrease in TNFR1 expression may

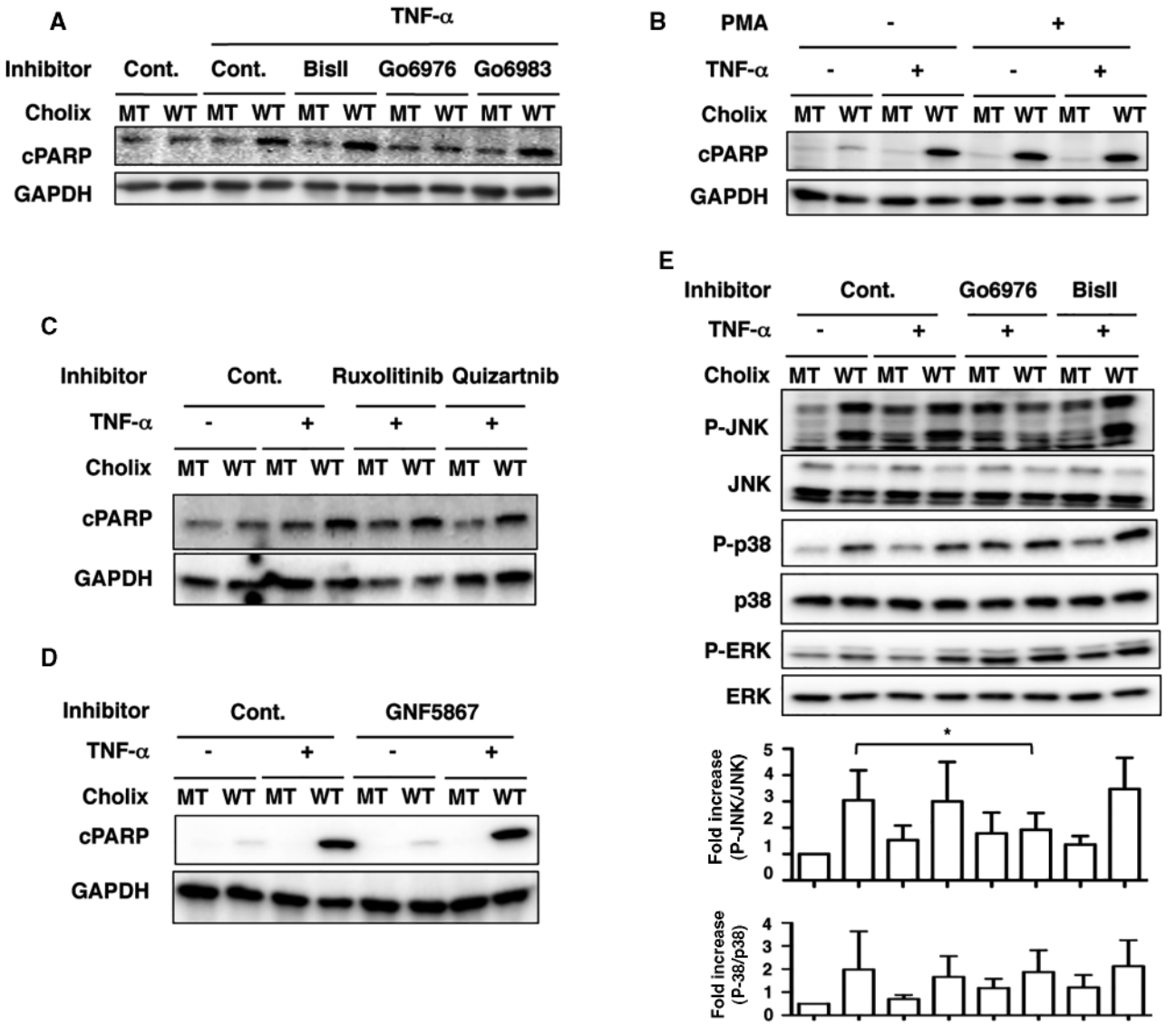

FIG. 6. Effect of protein kinase C inhibitors on HepG2 cells treated with TNF-α/Cholix. A–D, HepG2 cells (2×10^5 cells/well) were pretreated for 30 min with 5 μM PKC inhibitors (e.g., Bis II, Go6976, Go6983), 100 nM PMA, 20 μM SB20350, 10 μM Ruxolitinib, 10 μM Quizarnib, 10 μM GNF5867, followed by the incubation for 12 h with 10 μg/ml wild-type (WT) or mutant Cholix (MT) in the presence or absence of TNF-α (25 ng/ml). E, Cells were pretreated for 30 min with the indicated inhibitors and then incubated for 12 h with 10 μg/ml wild-type Cholix (WT) or mutant Cholix (MT) in the presence or absence of TNF-α (25 ng/ml). Then cells were lysed with 1×SDS sample buffer for immunoblotting with the indicated antibodies. Experiments were repeated three times with similar results. Quantification of phospho-JNK and phospho-p38 level in HepG2 cells was performed by densitometry (bottom panel). Data are presented as mean ±SD from three experiments and significance is *$P<0.05$.

occur thorough proteolytic degradation via the proteasome, and not through the lysosome.

MAP kinase signal transduction pathways are regulated by p38-MAPK, ERK, JNK, and ERK5. The MAP kinase pathway is involved in cell proliferation, differentiation, migration, senescence, and apoptosis (Sun *et al.*, 2015). In the absence of TNF-α, Cholix activated the MAPK pathway. Wätjen *et al.* (2014) reported in rat hepatocytes (H4IIE), that incubation with mycotoxin beauvericin increased JNK phosphorylation, decreased ERK phosphorylation and resulted in apoptosis. In rat intestinal (IEC-6) cells, TNF-α/cycloheximide-induced apoptosis was caused by ROS production, followed by phosphorylation of JNK and, subsequently, ERK (Jin *et al.*, 2008). Inhibition of Rac1 signaling by expression of dominant-negative Rac1 decreased TNF-α-induced mitochondrial ROS production (Jin *et al.*, 2008). In this study, TNF-α/Cholix-induced apoptotic signals were suppressed by specific inhibitors (Figs. 5 and 6), which interfered with Cholix-induced phosphorylation of JNK and ERK. PKC-activator, PMA, enhanced Cholix-induced PARP cleavage similar to what was seen by addition of TNF-α. It was reported that, in gastric cancer cells, PMA promoted PKC-dependent JNK activation, followed by induction of apoptosis (Chen *et al.*, 2002). In addition, PKC isoforms are involved in JNK activation, which induces apoptosis (Comalada *et al.*, 2003; Garin *et al.*, 2007; Lopez-Bergami and Ronai, 2008). Although we could not identify the PKC isoforms that regulate JNK activation, our data suggest that PKC regulates JNK activity, which is required for TNF-α/Cholix-induced apoptosis.

Furthermore, ROS inhibitor NAC pretreatment significantly suppressed apoptotic signals and phosphorylation of p38, JNK, and Akt, but not ERK. We also show here that TNF-α alone did not induce MAPK phosphorylation and HepG2 cell death.

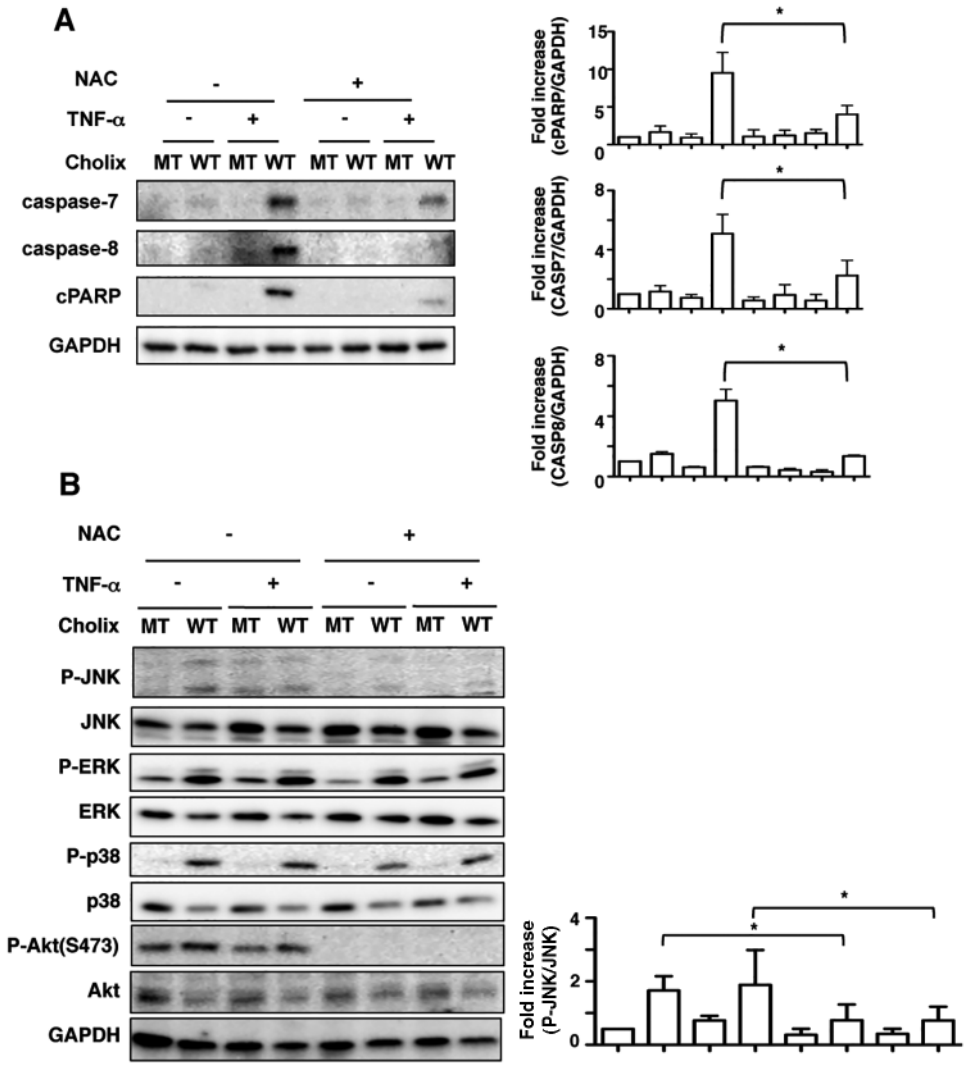

FIG. 7. ROS inhibitor suppresses TNF-α/Cholix-induced apoptotic signaling. A, Cells were pretreated for 30 min with or without 10 mM NAC, and then incubated for 12 h with wild-type Cholix (WT) or mutant Cholix(E581A) (MT) in the presence or absence of TNF-α. Then, cells were lysed with 1×SDS sample buffer for immunoblotting with the indicated antibodies. A blot representative of three separate experiments is shown. Quantification of TNF-α/Cholix-induced caspase-7, -8, and PARP cleavage levels in HepG2 cells was performed by densitometry (right panel). Data are presented as mean ±SD from three experiments and significance is *$P<0.05$. B, Cells were pretreated for 30 min with or without 10 mM NAC, and then incubated for 12 h with wild-type Cholix (WT) or mutant Cholix(E581A) (MT) in the presence or absence of TNF-α. Then, cells were lysed with 1×SDS sample buffer for immunoblotting with the indicated antibodies. A blot representative of three separate experiments is shown. Quantification of phospho-JNK level in HepG2 cells was performed by densitometry (right panel). Data are presented as mean ±SD from three experiments and significance is *$P<0.05$.

Further, TNFR1 knockdown decreased TNF-α/Cholix-induced PARP cleavage. Our data suggest that JNK is a key factor and ROS signals induced by the addition of TNF-α initiates cell death by TNF-α/Cholix, which is in agreement with a previous report; ROS and JNK pathways are important for TNF-α-mediated liver injury (Schwabe and Brenner, 2006). Thus, TNF-α acts as a key activator in Cholix-induced cell death. Kim *et al.* (2010) reported that ROS modulator 1 (Romo1) and B-cell lymphoma-extra large are directly associated with TNF-α/cycloheximide-induced ROS production in HeLa cells. TNF-α/Cholix-induced PARP cleavage was not suppressed in Romo1-overexpressing HepG2 cells (data not shown), indicating that Romo1 is not involved in TNF-α/Cholix-induced apoptosis.

In HepG2 cells, PARP cleavage and caspase activation were significantly enhanced by TNF-α/Cholix co-treatment (Figure 2 and Supplementary Figure 1C). Although a general caspase inhibitor, Z-VAD-Fmk, suppressed activation of caspases, cell viability was still reduced. Akt inhibitor pretreatment showed enhanced TNF-α/Cholix-induced apoptotic pathway. As shown in Figure 3D, TNF-α/Cholix-induced cell death was significantly improved by co-pretreatment with Z-VAD-Fmk and Akt inhibitor, Akti. Our data indicated that Akt activation might be induced by TNF-α/Cholix and is involved in non-apoptotic cell death. Previous reports showed that Akt activation induces necroptosis, a non-apoptotic programmed cell death. McNamara *et al.* (2013) reported that Akt controls necroptosis through downstream targeting of mammalian Target of Rapamycin complex 1 (mTORC1) in a RIP1-dependent fashion in mouse L929 fibroblasts. In mouse hippocampal HT22 cells, TNF-α/Z-VAD-Fmk co-treatment induced necroptosis, which was preceded by RIP1-RIP3-pAkt assembly (Liu *et al.*, 2014). Necroptosis has been considered as an alternative cell death mechanism, which is induced when apoptosis is blocked (Degterev *et al.*, 2005). In addition, a recent study showed that xenoestrogen

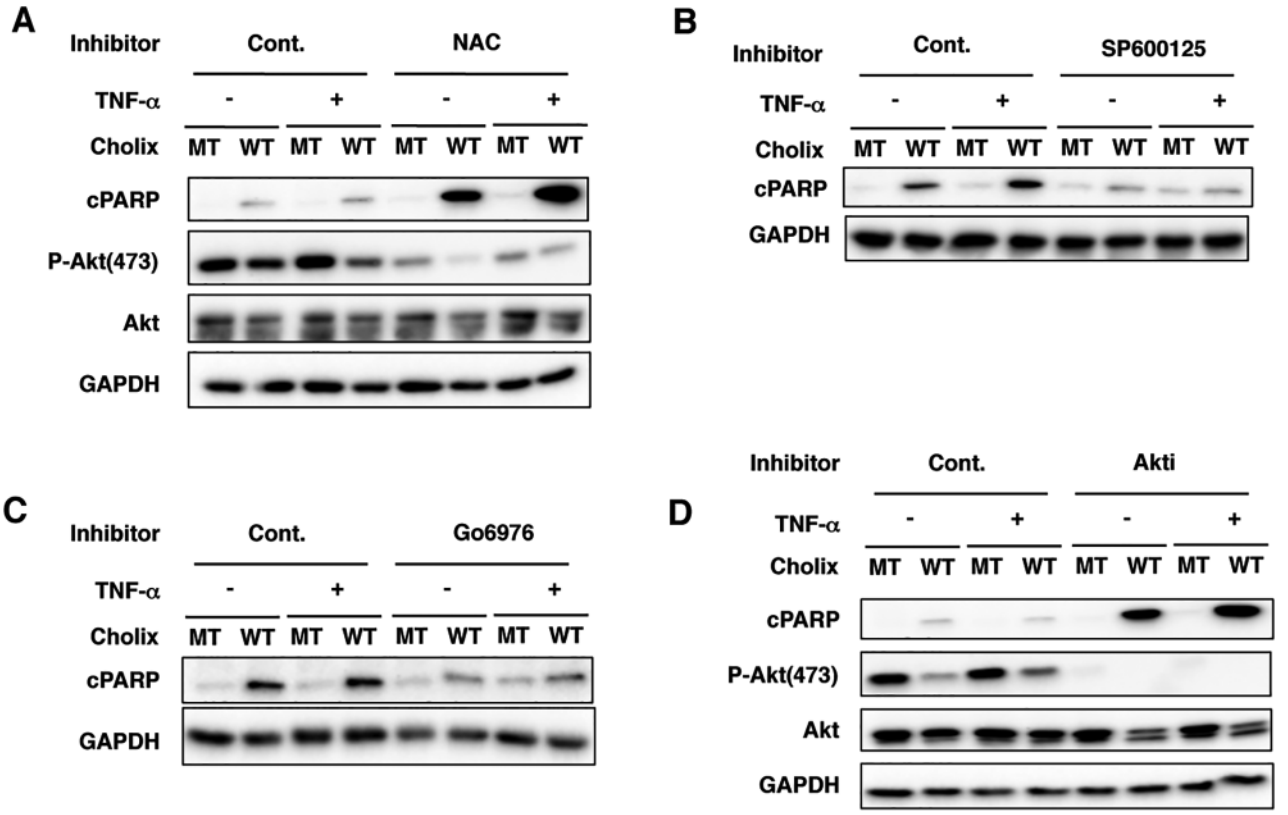

FIG. 8. Cholix-induced PARP cleavage is not enhanced by TNF-α in immortalized human hepatocytes. A–D, Immortalized human hepatocytes were pretreated with or without the inhibitors for 30 min, and then incubated for 12 h with wild-type Cholix (WT) or mutant Cholix(E581A) (MT) in the presence or absence of TNF-α. Then, cells were lysed with 1×SDS sample buffer for immunoblotting with the indicated antibodies. A blot representative of three separate experiments is shown.

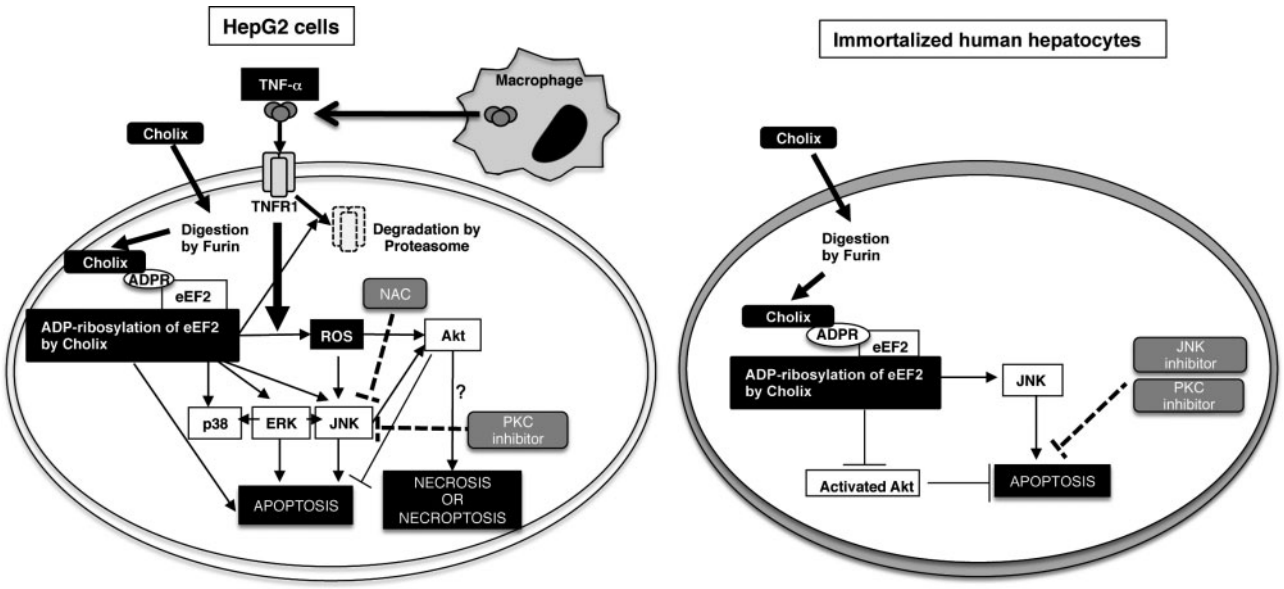

FIG. 9. Proposed model of TNF-α/Cholix-induced apoptotic signals in HepG2 cells and immortalized human hepatocytes. This figure is described in "Discussion".

4-nonylphenol reactivates ROS-dependent JNK- and AKT/AMPK/mTOR signaling, which regulates apoptosis, autophagy and necrosis (Duan *et al.*, 2016). Further, it was reported that JNK activation not only involves necroptosis (Chen *et al.*, 2011; Christofferson *et al.*, 2012) but also necrosis (Ventura *et al.*, 2004). Our result showed that inhibition of JNK phosphorylation by NAC or SP600125 suppressed TNF-α/Cholix-induced Akt phosphorylation in HepG2 cells, suggesting that Akt was regulated downstream of ROS and JNK, and that pathway might participate in cell death involving apoptosis, necroptosis or necrosis.

In contrast, it is also known that Akt activation protects liver from cell death during various stresses (e.g., acute cold

exposure, ischemia/reperfusion injury, cytokine) (Ashare *et al.*, 2007; Harada *et al.*, 2004; Wang *et al.*, 2013). In agreement with these previous reports, Cholix decreased Akt phosphorylation and Akt inhibitor increased Cholix-induced PARP cleavage in human immortalized hepatocytes, which are highly sensitive to Cholix and more responsive than HepG2 cells. These results indicate that, in human immortalized hepatocytes, Akt protects against Cholix-induced cytotoxicity.

In conclusion, we propose a model of TNF-α/Cholix-induced HepG2 cell death (Figure 9, left panel). Cholix is activated by Furin and induces eEF2 ADP-ribosylation. This event causes MAPK activation and Akt phosphorylation, followed by induction of apoptosis. In the presence of TNF-α from macrophages, TNF-α binds to TNFR1, and its signal leads to ROS production, and then MAPK activation in the presence of Cholix, but not TNF-α/Cholix(E581A). Inhibition of ROS by NAC suppressed phosphorylation of Akt and JNK. In addition, PKC inhibitor Go6973 suppressed TNF-α-enhanced JNK activation, suggesting that JNK regulates TNF-α/Cholix-induced cell death involving apoptosis, necroptosis or necrosis. On the contrary, in human immortalized hepatocytes (Figure 9, right panel), Cholix induced eEF2 ADP-ribosylation, followed by down-regulation of Akt phosphorylation. Addition of TNF-α did not affect Cholix-induced apoptosis. Inhibition of Akt activity by Akti or NAC promoted apoptosis by Cholix. Further, Cholix-induced apoptosis was suppressed by inhibition of JNK and PKC. Thus, the Cholix-induced cell death mechanism is different in HepG2 cells and immortalized human hepatocytes. We need further study to clarify this point. Taken together, our data show that TNF-α enhanced Cholix-induced apoptosis via MAPK activation in HepG2 cells.

SUPPLEMENTARY DATA

Supplementary data are available at *Toxicological Sciences* online.

ACKNOWLEDGMENTS

We thank Dr Tatsuo Kanda and Dr Ranjit Ray for kindly providing immortalized human hepatocytes. We acknowledge K. Hirano and T. Arai for their technical assistance.

FUNDING

Grant-in-Aid for Young Scientists from Japan Society for the Promotion of Science to K.O. (No. 24790409), Scientific Research from the Ministry of Education, Science and Culture of Japan to K.Y. (No. 25460526), Improvement of Research Environment for Young Researchers from Japan Science and Technology Agency, and Japan Agency for Medical Research and Development. J.M. was supported by the Intramural Research Program, National Institutes of Health, National Heart, Lung, and Blood Institute.

REFERENCES

Ashare, A., Monick, M. M., Nymon, A. B., Morrison, J. M., Noble, M., Powers, L. S., Yarovinsky, T. O., Yahr, T. L., and Hunninghake, G. W. (2007). *Pseudomonas aeruginosa* delays Kupffer cell death via stabilization of the X-chromosome-linked inhibitor of apoptosis protein. *J. Immunol.* **179**, 505–513.

Awasthi, S. P., Asakura, M., Chowdhury, N., Neogi, S. B., Hinenoya, A., Golbar, H. M., Yamate, J., Arakawa, E., Tada, T., Ramamurthy, T., *et al.* (2013). Novel cholix toxin variants, ADP-ribosylating toxins in *Vibrio cholerae* non-O1/non-O139 strains, and their pathogenicity. *Infect. Immun.* **81**, 531–541. 10.1128/IAI.00982-12.

Baud, V., and Karin, M. (2001). Signal transduction by tumor necrosis factor and its relatives. *Trends Cell Biol.* **11**, 372–377.

Behrens, M. M., Strasser, U., and Choi, D. W. (1999). Go 6976 is a potent inhibitor of neurotrophin-receptor intrinsic tyrosine kinase. *J. Neurochem.* **72**, 919–924.

Burvall, K., Palmberg, L., Larsson, K. (2005). Expression of TNFalpha and its receptors R1 and R2 in human alveolar epithelial cells exposed to organic dust and the effects of 8-bromo-cAMP and protein kinase A modulation. *Inflammat. Res.: Off. J. Eur. Histamine Res. Soc. ... [et al.]* **54**, 281–288. 10.1007/s00011-005-1356-7.

Chang, Q., and Tepperman, B. L. (2001). The role of protein kinase C isozymes in TNF-alpha-induced cytotoxicity to a rat intestinal epithelial cell line. *Am. J. Physiol. Gastrointest. Liver Physiol.* **280**, G572–G583.

Chen, G., and Goeddel, D. V. (2002). TNF-R1 signaling: a beautiful pathway. *Science* **296**, 1634–1635. 10.1126/science.1071924.

Chen, M., Guerrero, A. D., Huang, L., Shabier, Z., Pan, M., Tan, T. H., and Wang, J. (2007). Caspase-9-induced mitochondrial disruption through cleavage of anti-apoptotic BCL-2 family members. *J. Biol. Chem.* **282**, 33888–33895. 10.1074/jbc.M702969200.

Chen, S. Y., Chiu, L. Y., Maa, M. C., Wang, J. S., Chien, C. L., and Lin, W. W. (2011). zVAD-induced autophagic cell death requires c-Src-dependent ERK and JNK activation and reactive oxygen species generation. *Autophagy* **7**, 217–228.

Chen, Y., Wu, Q., Song, S. Y., and Su, W. J. (2002). Activation of JNK by TPA promotes apoptosis via PKC pathway in gastric cancer cells. *World J. Gastroenterol.* **8**, 1014–1018.

Chin, Y. R., and Horwitz, M. S. (2005). Mechanism for removal of tumor necrosis factor receptor 1 from the cell surface by the adenovirus RIDalpha/beta complex. *J. Virol.* **79**, 13606-17. 10.1128/JVI.79.21.13606-13617.2005.

Chiron, M. F., Fryling, C. M., and FitzGerald, D. (1997). Furin-mediated cleavage of Pseudomonas exotoxin-derived chimeric toxins. *J. Biol. Chem.* **272**, 31707–31711.

Chiu, C. C., Chen, H. H., Chuang, H. L., Chung, T. C., Chen, S. D., and Huang, Y. T. (2009). *Pseudomonas aeruginosa* exotoxin A-induced hepatotoxicity: an animal model in rats. *J. Veterin. Med. Sci./Jpn. Soc. Veterin. Sci.* **71**, 1–8.

Cho, S. W., Hartle, L., Son, S. M., Yang, F., Goldberg, M., Xu, Q., Langer, R., and Anderson, D. G. (2008). Delivery of small interfering RNA for inhibition of endothelial cell apoptosis by hypoxia and serum deprivation. *Biochem. Biophys. Res. Commun.* **376**, 158–163. 10.1016/j.bbrc.2008.08.123.

Cho, Y. S., Challa, S., Moquin, D., Genga, R., Ray, T. D., Guildford, M., and Chan, F. K. (2009). Phosphorylation-driven assembly of the RIP1-RIP3 complex regulates programmed necrosis and virus-induced inflammation. *Cell* **137**, 1112–1123. 10.1016/j.cell.2009.05.037.

Christofferson, D. E., Li, Y., Hitomi, J., Zhou, W., Upperman, C., Zhu, H., Gerber, S. A., Gygi, S., and Yuan, J. (2012). A novel role for RIP1 kinase in mediating TNFalpha production. *Cell Death Dis.* **3**, e320. 10.1038/cddis.2012.64.

Comalada, M., Xaus, J., Valledor, A. F., Lopez-Lopez, C., Pennington, D. J., and Celada, A. (2003). PKC epsilon is involved in JNK activation that mediates LPS-induced TNF-alpha, which induces apoptosis in macrophages. *Am. J. Physiol. Cell Physiol.* **285**, C1235–C1245. 10.1152/ajpcell.00228.2003.

Croft, M., Duan, W., Choi, H., Eun, S. Y., Madireddi, S., and Mehta, A. (2012). TNF superfamily in inflammatory disease: translating basic insights. *Trends Immunol.* **33**, 144–152. 10.1016/j.it.2011.10.004.

Degterev, A., Huang, Z., Boyce, M., Li, Y., Jagtap, P., Mizushima, N., Cuny, G. D., Mitchison, T. J., Moskowitz, M. A., and Yuan, J. (2005). Chemical inhibitor of nonapoptotic cell death with therapeutic potential for ischemic brain injury. *Nat. Chem. Biol.* **1**, 112–119. 10.1038/nchembio711.

Devin, A., Lin, Y., Yamaoka, S., Li, Z., Karin, M., and Liu, Z. (2001). The alpha and beta subunits of IkappaB kinase (IKK) mediate TRAF2-dependent IKK recruitment to tumor necrosis factor (TNF) receptor 1 in response to TNF. *Mol. Cell. Biol.* **21**, 3986–3994. 10.1128/MCB.21.12.3986-3994.2001.

Duan, P., Hu, C., Quan, C., Yu, T., Zhou, W., Yuan, M., Shi, Y., and Yang, K. (2016). 4-Nonylphenol induces apoptosis, autophagy and necrosis in Sertoli cells: involvement of ROS-mediated AMPK/AKT-mTOR and JNK pathways. *Toxicology* **341-343**, 28–40. 10.1016/j.tox.2016.01.004.

Garin, G., Abe, J., Mohan, A., Lu, W., Yan, C., Newby, A. C., Rhaman, A., and Berk, B. C. (2007). Flow antagonizes TNF-alpha signaling in endothelial cells by inhibiting caspase-dependent PKC zeta processing. *Circ. Res.* **101**, 97–105, 10.1161/CIRCRESAHA.107.148270.

Grandage, V. L., Everington, T., Linch, D. C., and Khwaja, A. (2006). Go6976 is a potent inhibitor of the JAK 2 and FLT3 tyrosine kinases with significant activity in primary acute myeloid leukaemia cells. *Br. J. Haematol.* **135**, 303–316. 10.1111/j.1365-2141.2006.06291.x.

Gschwendt, M., Dieterich, S., Rennecke, J., Kittstein, W., Mueller, H. J., and Johannes, F. J. (1996). Inhibition of protein kinase C mu by various inhibitors. Differentiation from protein kinase c isoenzymes. *FEBS Lett.* **392**, 77–80.

Gu, M., Gordon, V. M., Fitzgerald, D. J., and Leppla, S. H. (1996). Furin regulates both the activation of *Pseudomonas exotoxin* A and the quantity of the toxin receptor expressed on target cells. *Infect. Immun.* **64**, 524–527.

Harada, N., Hatano, E., Koizumi, N., Nitta, T., Yoshida, M., Yamamoto, N., Brenner, D. A., and Yamaoka, Y. (2004). Akt activation protects rat liver from ischemia/reperfusion injury. *J. Surg. Res.* **121**, 159–170. 10.1016/j.jss.2004.04.016.

Hasan, N. A., Choi, S. Y., Eppinger, M., Clark, P. W., Chen, A., Alam, M., Haley, B. J., Taviani, E., Hine, E., Su, Q., *et al.* (2012). Genomic diversity of 2010 Haitian cholera outbreak strains. *Proc. Natl Acad. Sci. USA.* **109**, E2010–E2017. 10.1073/pnas.1207359109.

Hosaka, M., Nagahama, M., Kim, W. S., Watanabe, T., Hatsuzawa, K., Ikemizu, J., Murakami, K., and Nakayama, K. (1991). Arg-X-Lys/Arg-Arg motif as a signal for precursor cleavage catalyzed by furin within the constitutive secretory pathway. *J. Biol. Chem.* **266**, 12127–12130.

Hughes, J. M., Hollis, D. G., Gangarosa, E. J., and Weaver, R. E. (1978). Non-cholera vibrio infections in the United States. Clinical, epidemiologic, and laboratory features. *Ann. Internal Med.* **88**, 602-6.

Iglewski, B. H., Liu, P. V., and Kabat, D. (1977). Mechanism of action of *Pseudomonas aeruginosa* exotoxin Aiadenosine diphosphate-ribosylation of mammalian elongation factor 2 in vitro and in vivo. *Infect. Immun.* **15**, 138–144.

Inocencio, N. M., Moehring, J. M., and Moehring, T. J. (1994). Furin activates *Pseudomonas exotoxin* A by specific cleavage in vivo and in vitro. *J. Biol. Chem.* **269**, 31831–31835.

Jin, S., Ray, R. M., and Johnson, L. R. (2008). TNF-alpha/cycloheximide-induced apoptosis in intestinal epithelial cells requires Rac1-regulated reactive oxygen species. *Am. J. Physiol. Gastrointestinal Liver Physiol.* **294**, G928–G937. 10.1152/ajpgi.00219.2007.

Jorgensen, R., Purdy, A. E., Fieldhouse, R. J., Kimber, M. S., Bartlett, D. H., and Merrill, A. R. (2008). Cholix toxin, a novel ADP-ribosylating factor from *Vibrio cholerae*. *J. Biol. Chem.* **283**, 10671–10678. 10.1074/jbc.M710008200.

Kaper, J. B., Morris, J. G., Jr., and Levine, M. M. (1995). Cholera. *Clin. Microbiol. Rev.* **8**, 48–86.

Khan, S., Kumar, A., Meparambu, D., Thomas, S., Harichandran, D., and Karim, S. (2013). Fatal non-O1, non-O139 *Vibrio cholerae* septicaemia in a patient with chronic liver disease. *J. Med. Microbiol.* **62**, 917–921. 10.1099/jmm.0.049296-0.

Kim, J. J., Lee, S. B., Park, J. K., and Yoo, Y. D. (2010). TNF-alpha-induced ROS production triggering apoptosis is directly linked to Romo1 and Bcl-X(L). *Cell Death Differ.* **17**, 1420–1434. 10.1038/cdd.2010.19.

Liedtke, C., Plumpe, J., Kubicka, S., Bradham, C. A., Manns, M. P., Brenner, D. A., and Trautwein, C. (2002). Jun kinase modulates tumor necrosis factor-dependent apoptosis in liver cells. *Hepatology* **36**, 315–325. 10.1053/jhep.2002.34615.

Liu, Q., Qiu, J., Liang, M., Golinski, J., van Leyen, K., Jung, J. E., You, Z., Lo, E. H., Degterev, A., and Whalen, M. J. (2014). Akt and mTOR mediate programmed necrosis in neurons. *Cell Death Dis.* **5**, e1084. 10.1038/cddis.2014.69.

Liu, S., Milne, G. T., Kuremsky, J. G., Fink, G. R., and Leppla, S. H. (2004). Identification of the proteins required for biosynthesis of diphthamide, the target of bacterial ADP-ribosylating toxins on translation elongation factor 2. *Mol. Cell. Biol.* **24**, 9487-97. 10.1128/MCB.24.21.9487-9497.2004.

Lopez-Bergami, P., Habelhah, H., Bhoumik, A., Zhang, W., Wang, L. H., and Ronai, Z. (2005). RACK1 mediates activation of JNK by protein kinase C [corrected]. *Mol. Cell* **19**, 309–320. 10.1016/j.molcel.2005.06.025.

Lopez-Bergami, P., and Ronai, Z. (2008). Requirements for PKC-augmented JNK activation by MKK4/7. *Int. J. Biochem. Cell Biol.* **40**, 1055–1064. 10.1016/j.biocel.2007.11.011.

Martiny-Baron, G., Kazanietz, M. G., Mischak, H., Blumberg, P. M., Kochs, G., Hug, H., Marme, D., and Schachtele, C. (1993). Selective inhibition of protein kinase C isozymes by the indolocarbazole Go 6976. *J. Biol. Chem.* **268**, 9194–9197.

McNamara, C. R., Ahuja, R., Osafo-Addo, A. D., Barrows, D., Kettenbach, A., Skidan, I., Teng, X., Cuny, G. D., Gerber, S., and Degterev, A. (2013). Akt Regulates TNFalpha synthesis downstream of RIP1 kinase activation during necroptosis. *PloS One* **8**, e56576. 10.1371/journal.pone.0056576.

Morinaga, N., Yahiro, K., Matsuura, G., Moss, J., and Noda, M. (2008). Subtilase cytotoxin, produced by Shiga-toxigenic *Escherichia coli*, transiently inhibits protein synthesis of Vero cells via degradation of BiP and induces cell cycle arrest at G1 by downregulation of cyclin D1. *Cell. Microbiol.* **10**, 921–929. 10.1111/j.1462-5822.2007.01094.x.

Morris, J. G., Jr., and Black, R. E. (1985). Cholera and other vibrioses in the United States. *N. Eng. J. Med.* **312**, 343–350. 10.1056/NEJM198502073120604.

Mosselmans, R., Hepburn, A., Dumont, J. E., Fiers, W., and Galand, P. (1988). Endocytic pathway of recombinant murine tumor necrosis factor in L-929 cells. *J. Immunol.* **141**, 3096–3100.

Muhlen, K. A., Schumann, J., Wittke, F., Stenger, S., Van Rooijen, N., Van Kaer, L., and Tiegs, G. (2004). NK cells, but not NKT cells, are involved in *Pseudomonas aeruginosa* exotoxin A-induced hepatotoxicity in mice. *J. Immunol.* **172**, 3034–3041.

Ogura, K., Yahiro, K., Tsutsuki, H., Nagasawa, S., Yamasaki, S., Moss, J., and Noda, M. (2011). Characterization of Cholix toxin-induced apoptosis in HeLa cells. *J. Biol. Chem.* **286**, 37207–37215. 10.1074/jbc.M111.246504.

Parameswaran, N., and Patial, S. (2010). Tumor necrosis factor-alpha signaling in macrophages. *Crit. Rev. Eukaryotic Gene Express.* **20**, 87–103.

Patel, N. M., Wong, M., Little, E., Ramos, A. X., Kolli, G., Fox, K. M., Melvin, J., Moore, A., and Manch, R. (2009). *Vibrio cholerae* non-O1 infection in cirrhotics: case report and literature review. *Transplant Infect. Dis.: Off. J. Transplant. Soc.* **11**, 54–56. 10.1111/j.1399-3062.2008.00339.x.

Purdy, A. E., Balch, D., Lizarraga-Partida, M. L., Islam, M. S., Martinez-Urtaza, J., Huq, A., Colwell, R. R., and Bartlett, D. H. (2010). Diversity and distribution of cholix toxin, a novel ADP-ribosylating factor from *Vibrio cholerae*. *Environ. Microbiol. Rep.* **2**, 198–207. 10.1111/j.1758-2229.2010.00139.x.

Ray, R. B., Meyer, K., and Ray, R. (2000). Hepatitis C virus core protein promotes immortalization of primary human hepatocytes. *Virology* **271**, 197–204. 10.1006/viro.2000.0295.

Roy, V., Ghani, K., and Caruso, M. (2010). A dominant-negative approach that prevents diphthamide formation confers resistance to *Pseudomonas exotoxin* A and diphtheria toxin. *PloS One* **5**, e15753. 10.1371/journal.pone.0015753.

Schumann, J., Angermuller, S., Bang, R., Lohoff, M., and Tiegs, G. (1998). Acute hepatotoxicity of *Pseudomonas aeruginosa* exotoxin A in mice depends on T cells and TNF. *J. Immunol.* **161**, 5745–5754.

Schumann, J., Wolf, D., Pahl, A., Brune, K., Papadopoulos, T., van Rooijen, N., and Tiegs, G. (2000). Importance of Kupffer cells for T-cell-dependent liver injury in mice. *Am. J. Pathol.* **157**, 1671–1683. 10.1016/S0002-9440(10)64804-3.

Schwabe, R. F., and Brenner, D. A. (2006). Mechanisms of Liver Injury. I. TNF-alpha-induced liver injury: role of IKK, JNK, and ROS pathways. *Am. J. Physiol. Gastrointest. Liver Physiol.* **290**, G583–G589. 10.1152/ajpgi.00422.2005.

Sun, Y., Liu, W. Z., Liu, T., Feng, X., Yang, N., and Zhou, H. F. (2015). Signaling pathway of MAPK/ERK in cell proliferation, differentiation, migration, senescence and apoptosis. *J. Receptor Signal Transduct. Res.* **35**, 600–604. 10.3109/10799893.2015.1030412.

Ventura, J. J., Cogswell, P., Flavell, R. A., Baldwin, A. S., Jr., and Davis, R. J. (2004). JNK potentiates TNF-stimulated necrosis by increasing the production of cytotoxic reactive oxygen species. *Genes Dev.* **18**, 2905–2915. 10.1101/gad.1223004.

Wajant, H., Pfizenmaier, K., and Scheurich, P. (2003). Tumor necrosis factor signaling. *Cell Death Differ.* **10**, 45–65. 10.1038/sj.cdd.4401189.

Wang, J., Chen, Y., Zhang, W., Zheng, G., Meng, S., Che, H., Ke, T., Yang, J., Chen, J., and Luo, W. (2013). Akt activation protects liver cells from apoptosis in rats during acute cold exposure. *Int. J. Biol. Sci.* **9**, 509–517. 10.7150/ijbs.5220.

Watjen, W., Debbab, A., Hohlfeld, A., Chovolou, Y., and Proksch, P. (2014). The mycotoxin beauvericin induces apoptotic cell death in H4IIE hepatoma cells accompanied by an inhibition of NF-kappaB-activity and modulation of MAP-kinases. *Toxicol. Lett.* **231**, 9–16. 10.1016/j.toxlet.2014.08.021.

Zhang, S. Q., Kovalenko, A., Cantarella, G., and Wallach, D. (2000). Recruitment of the IKK signalosome to the p55 TNF receptor: RIP and A20 bind to NEMO (IKKgamma) upon receptor stimulation. *Immunity* **12**, 301–311.